Journal of Power Sources 195 (2010) 7098–7101

Contents lists available at ScienceDirect

Journal of Power Sources

journal homepage: www.elsevier.com/locate/jpowsour

Short communication

Synthesis of single crystalline $Li_{0.44}MnO_2$ nanowires with large specific capacity and good high current density property for a positive electrode of Li ion battery

Eiji Hosono[a], Hirofumi Matsuda[a], Tatsuya Saito[a], Tetsuichi Kudo[a], Masaki Ichihara[b], Itaru Honma[a], Haoshen Zhou[a,*]

[a] National Institute of Advanced Industrial Science and Technology, Umezono, 1-1-1, Tsukuba 305-8568, Japan
[b] Material Design and Characterization Laboratory Institute for Solid State Physics, University of Tokyo, 5-1-5, Kashiwanoha, Kashiwa, Chiba 277-8581, Japan

ARTICLE INFO

Article history:
Received 2 October 2009
Received in revised form 16 February 2010
Accepted 28 April 2010
Available online 4 May 2010

Keywords:
$Li_{0.44}MnO_2$
Single crystal
Nanowire
Li ion battery

ABSTRACT

The fabrication of single crystalline $Li_{0.44}MnO_2$ nanowires for the positive electrode of lithium ion battery is reported. The single crystalline $Li_{0.44}MnO_2$ nanowires are obtained by lithium exchange reaction of $Na_{0.44}MnO_2$ nanowires with high aspect ratio. The $Li_{0.44}MnO_2$ nanowires indicate both the large specific capacity of around 250 mAh g^{-1} (1.5–4.5 V vs. Li/Li^+) and the good high current density property for the positive electrode of lithium ion battery.

1. Introduction

Lithium storage devices have been widely studied for the portable electric device and the electric vehicle (EV) or hybrid EV (HEV). These lithium storage devices need both large specific capacity and high rate charge–discharge performances. Up to now, the increase of the specific capacity of a negative electrode has been reported by using alloy compounds such as Si and Sn [1,2], transition metal oxides nanoparticles [3]. However, in the case of positive electrode, the increase of the specific capacity is still remained as important problems. Generally, it is difficult to take the traditional positive electrode materials such as $LiCoO_2$ for EV and HEV due to its low specific capacity and high cost problems. Of course, the low specific capacity of most positive electrode active materials cannot satisfy the increasing industry needs. Vanadium compounds such as V_2O_5 [4,5] and manganese compounds [6–8] have been attracted by researchers due to the low cost materials and large capacity.

For development of the high rate performance (large current density), nanostructure controlled electrodes indicate good improvement [9–13]. The large surface area for interface reaction and the short diffusion distance of lithium ion are appropriate for the condition under high current density. The controversial point using nanoparticles is the aggregation, crystal growth and the safety problem. If the nanoparticles penetrated the separator in the battery, the cell would be broken. Therefore, the nanostructural control electrode such as one-dimensional nanowire is preferred than general nanoparticles. The nanowire structure does not cause the aggregation due to the nonwoven fabric structure constructed by the nanowires and penetration through the separator. The many manganese oxide nanowires such as MnO_2, Mn_3O_4, and MnOOH have been reported. [14–16]. Many Li–Mn oxides are unstable for lithium ion's insertion/extraction cycling by transferring into a spinel structure [17]. However, $Na_{0.44}MnO_2$ is interesting because the tunnel structure of $Na_{0.44}MnO_2$ prevents the conversion into spinel [17,18]. According to our knowledge, $Na_{0.44}MnO_2$ nanowires have not been reported up to our report [19]. Other reported $Na_{0.44}MnO_2$ wires are assembled by very thick bundle over several hundreds of μm [20,21] or sub-micron scale rod [22]. The bundle structure is not suitable for the fast charge–discharge Li ion battery, which need large surface area. Recently, we reported single crystalline $LiMn_2O_4$ nanowire via $Na_{0.44}MnO_2$ nanowire [23]. So, $Na_{0.44}MnO_2$ nanowire plays a role as self-template for other manganese oxide nanowire.

In this work, we report the single crystalline $Li_{0.44}MnO_2$ nanowires for the positive electrode of lithium ion battery. The single crystalline $Li_{0.44}MnO_2$ nanowires are obtained by lithium exchange reaction of $Na_{0.44}MnO_2$ nanowires with high aspect ratio. The $Li_{0.44}MnO_2$ nanowires indicate the large specific capacity of around 250 mAh g^{-1} for the positive electrode of lithium ion bat-

* Corresponding author. Tel.: +81 29 861 5795; fax: +81 29 861 5799.
E-mail address: hs.zhou@aist.go.jp (H. Zhou).

0378-7753/$ – see front matter © 2010 Elsevier B.V. All rights reserved.
doi:10.1016/j.jpowsour.2010.04.086

tery. Moreover, the nanowire structure indicates the good high current density property too.

2. Experimental

The 0.1 g of commercial Mn_3O_4 powders (Aldrich) were dispersed into the NaOH (Wako Chemical) aqueous solution (5 mol dm^{-3}) of 40 ml. It was placed in the Teflon-lined autoclave (Model 4744, Parr Instrument Company). The autoclave was heated at 205 °C for 4 days. The synthesis of $Na_{0.44}MnO_2$ nanowire has been reported [19]. After that, the synthesized $Na_{0.44}MnO_2$ was washed repeatedly by deionized water. The washed $Na_{0.44}MnO_2$ was dried at room temperature in the vacuum condition. The sodium/lithium ion exchange was performed in molten salts by $LiNO_3$ (Wako Chemical) (88 mol%) and LiCl (Wako Chemical) (12 mol%) at 300 °C for 10 h [22,23], which is different temperature with the process of single crystalline $LiMn_2O_4$ nanowire [23]. The sample was washed repeatedly by deionized water and dried at room temperature in the vacuum condition.

The crystal structure was examined by X-ray diffraction (XRD) analysis with a Bruker axs D8 Advance using Cu Kα radiation. The morphology of the film was examined by field-emission scanning electron microscopy (FESEM), high resolution transmission electron microscopy (HRTEM) using a Carl Zeiss Gemini Supra and a JEOL JEM-2010F.

Electrochemical measurements were performed by a three-electrode cell. The $Li_{0.44}MnO_2$ nanowires were mixed and ground with 5 wt% Teflon powder and 45 wt% acetylene black (the ratio of the acetylene black is larger than that of general battery on market because the appropriate mixing of one-dimensional active materials and carbon is difficult in the low ratio carbon condition. We think the improvement of the mixing process is next stage. In this work, we pay attention to the confirmation of natural property of the $Li_{0.44}MnO_2$ nanowires. In fact, the capacity of acetylene black is around 9–10 mAh g^{-1} at 0.1 A g^{-1}. The small capacity of acetylene black does not affect to the capacity of the electrode). The mixture was spread and pressed on the SUS-304 mesh as working electrode. The reference and counter electrodes were prepared by lithium metals on SUS-304 mesh. A 1 mol dm^{-3} $LiClO_4$ in EC/DEC was used as electrolyte. The weight in specific capacity (mAh g^{-1}) and current density (A g^{-1}) is calculated by only active materials.

3. Results and discussion

Fig. 1(a) and (b) shows an XRD pattern of the synthesized nanowires after low temperature hydrothermal treatment and the lithium exchanged nanowires in the flux at 300 °C for 10 h, respectively. The diffraction pattern of (a) agrees with that of $Na_4Mn_9O_{18}$ ($Na_{0.44}MnO_2$) in the JCPDS No. 27-0750. The orthorhombic lattice parameters were $a = 9.06(5)$ Å, $b = 26.39(3)$ Å, $c = 2.84(6)$ Å. The lithium exchange reaction is based on the report by Bruce et al. [24] and Akimoto et al. [25]. The pattern of lithium exchanged nanowires is similar to that of $Li_{0.44}MnO$ [23,25] with a tunnel structure. The lithium ion exchange in the flux results in the formation of $Li_{0.44}MnO_2$ from $Na_{0.44}MnO_2$.

Fig. 2(a) and (b) shows the SEM images of $Na_{0.44}MnO_2$ nanowires and $Li_{0.44}MnO_2$ nanowires, respectively. The morphology of the $Li_{0.44}MnO_2$ nanowires is similar to that of $Na_{0.44}MnO_2$ nanowires. The long nanowire morphology is not changed during flux reaction at 300 °C for 10 h to exchange the sodium in $Na_{0.44}MnO_2$ by the lithium to form $Li_{0.44}MnO_2$.

Fig. 3(a) shows the TEM image of the $Li_{0.44}MnO_2$ nanowires. The electron diffraction pattern in an inset image of Fig. 3(a) and the high resolution TEM image in Fig. 3(b) indicate that the $Li_{0.44}MnO_2$ nanowires are single crystalline nanowires to the

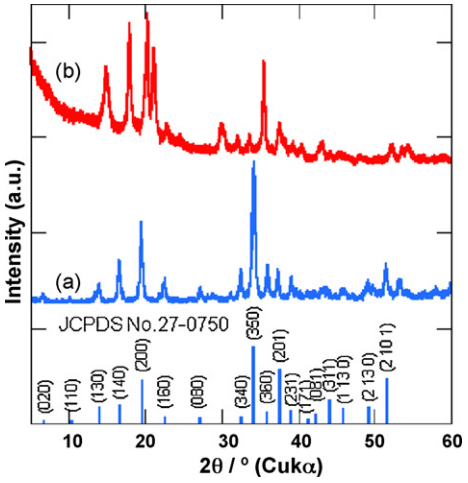

Fig. 1. (a) XRD pattern of the nanowires synthesized by the low temperature hydrothermal treatment. The pattern agrees with the $Na_{0.44}MnO_2$ (JCPDS: 27-0750). (b) XRD pattern of the nanowires obtained by lithium ion exchange of $Na_{0.44}MnO_2$ nanowires in flux. The pattern indicates the formation of $Li_{0.44}MnO_2$.

one-dimensional direction. According to the HRTEM and ED, the growth direction is [0 0 1] and the wall plane's direction is [*hk*0]. The one-dimensional direction of $Li_{0.44}MnO_2$ is similar to those of $Na_{0.44}MnO_2$ nanowires as shown in Fig. 4. The lithium site is exchanged from $Na_{0.44}MnO_2$. Generally, the $Li_{0.44}MnO_2$ are synthesized through only ion exchange reaction between sodium and lithium. The key point for synthesis of $Li_{0.44}MnO_2$ nanowires is the use of $Na_{0.44}MnO_2$ nanowires for ion exchange. The lithium

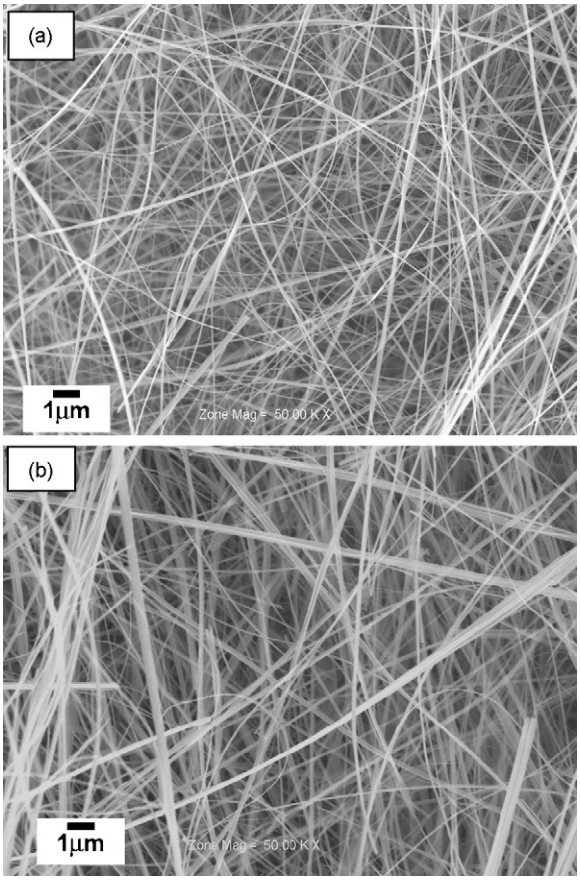

Fig. 2. (a and b) are SEM images of the $Na_{0.44}MnO_2$ nanowires and the $Li_{0.44}MnO_2$ nanowires, respectively.

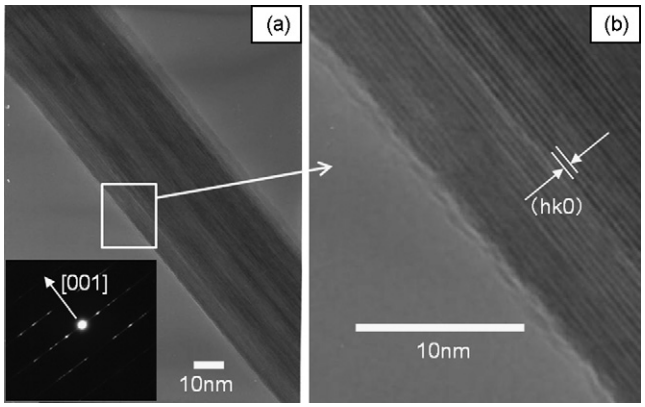

Fig. 3. (a) TEM image of the $Li_{0.44}MnO_2$ nanowires. The inset image is ED pattern of the $Li_{0.44}MnO_2$ nanowires. (b) High resolution TEM images of the $Li_{0.44}MnO_2$ nanowires. The lattice distance, which is parallel to the wall of the nanowire, is (*hk*0). The one-dimensional direction is [1 0 0]. The lattice image and ED pattern shows the single crystalline nature to one-dimensional direction.

storage properties of $Li_{0.44}MnO_2$ nanowires for positive electrode were investigated. Fig. 5(a) and (b) shows the first and second charge/discharge cycling curves at 0.1 A g^{-1}, 1 A g^{-1}, 5 A g^{-1} and 10 A g^{-1}, respectively. The measurement is started by charge condition. Although the charge capacity is around 55 mAh g^{-1} at 0.1 A g^{-1}, which means that about 0.19 Li is extracted from $Li_{0.44}MnO_2$ to reach $Li_{0.25}MnO_2$, the following discharge capacity is around 247 mAh g^{-1}, which means that about 0.82 Li is inserted into the $Li_{0.25}MnO_2$ to form $Li_{1.07}MnO_2$. Generally, the theoretical capacity is 131 mAh g^{-1} (0.44 Li/$Li_{0.44}MnO_2$). Here, a little exceed 1.0 Li is resulted from the EDLC of carbon and other effects. So, about 0.82 Li can be inserted/extracted into/from $Li_{0.44}MnO_2$ with capacity about 250 mAh g^{-1}. In the discharge curves at the current density of 0.1 A g^{-1}, three kinds of the plateau like shoulder at 4 V, 3 V and 2.5–2 V regions are observed. In the reported $Li_{0.44}MnO_2$ electrode, which are bulk crystals based on solid state reaction, two kinds of plateau at around 3.3 V and 3.1 V (Li/Li^+) are observed [18,24–26]. In all previous reports of $Li_{0.44}MnO_2$, the voltage window is over 2.5 V (Li/Li^+) because the curves rapidly decrease after the plateau at around 3.1 V. So, the existence of the shoulder at 2.5–2 V in Fig. 5 is the first report. The increase of the specific capacity and capacitor-like curves (plateau like shoulder) resulted from the nanostructure effect has been observed in other electrode

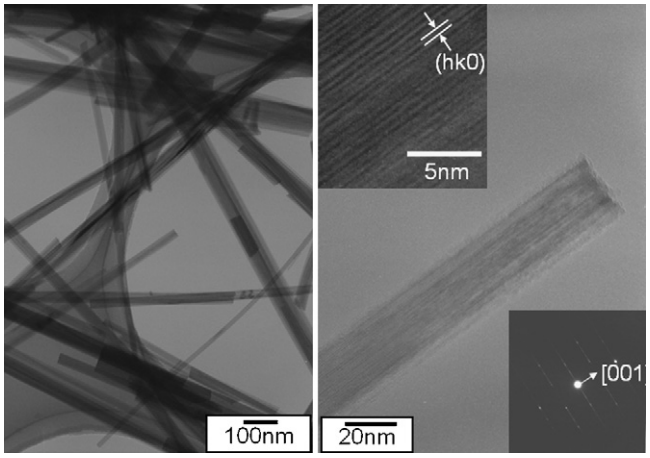

Fig. 4. (a) TEM image of the $Na_{0.44}MnO_2$ nanowires. (b) High resolution TEM images and ED pattern of the $Na_{0.44}MnO_2$ nanowires. The lattice distance, which is parallel to the wall of the nanowire, is (*hk*0) in inset image. The one-dimensional direction is [0 0 1]. The lattice image and ED pattern shows the single crystalline nature to one-dimensional direction.

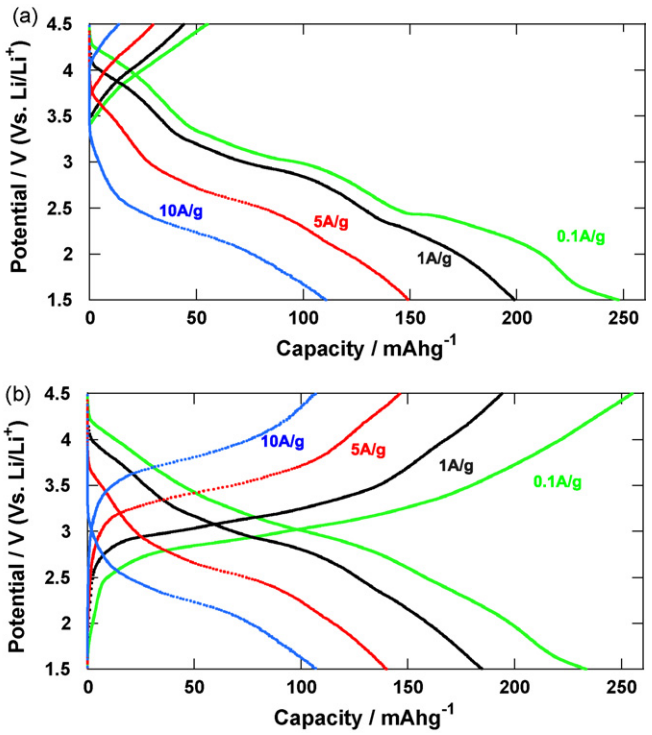

Fig. 5. The lithium storage characteristics of $Li_{0.44}MnO_2$ nanowires electrode at various current densities (0.1 A g^{-1} (0.1 C), 1 A g^{-1}(1 C), 5 A g^{-1}(5 C), 0 A g^{-1}(10 C). (a) First cycle and (b) second cycle. The current rate (1 C = 100 mA g^{-1}) is calculated by only active materials.

materials [10,27–29]. In our previous work, we also reported that the discharge curve of nanocrystalline $LiCoO_2$ indicates the novel capacitor behavior due to the distribution of the site energy by surface sites [30]. It is supposed that the capacitor-like behavior of $Li_{0.44}MnO_2$ nanowires is based on the similar reason by nanostructure. The specific discharge capacity of single crystalline $Li_{0.44}MnO_2$ nanowire is as large as around 230 mAh g^{-1} at second cycle.

The discharge capacities at high current density condition of 1 A g^{-1}, 5 A g^{-1} and 10 A g^{-1} are around 185 mAh g^{-1}, 140 mAh g^{-1} and 105 mAh g^{-1}, respectively, as shown in Fig. 5(b). The large discharge capacity is maintained in spite of the very high current density. The 140 mAh g^{-1} at 5 A g^{-1} is similar capacitor to a theoretical capacity of $LiCoO_2$, which is popular positive electrode. Fig. 6(a) shows the diagram for discharge capacity vs. cycle number for various current densities from 0.1 A g^{-1} to 10 A g^{-1}. At the 20th cycles, the discharge capacities at 0.1 A g^{-1}, 1 A g^{-1}, 5 A g^{-1} and 10 A g^{-1} are 143 mAh g^{-1}, 131 mAh g^{-1}, 107 mAh g^{-1} and 91 mAh g^{-1}, respectively. The cycle deterioration is decreased as increasing the current density from 0.1 A g^{-1} to 10 A g^{-1}.

Fig. 6(b) shows the diagram for discharge capacity vs. cycle number up to 100 cycles for extreme high current density at 5 A g^{-1} and 10 A g^{-1}. After the 100 cycles at even extreme high current density 5 A g^{-1} and 10 A g^{-1}, the capacities are 74 mAh g^{-1} and 74 mAh g^{-1}, respectively. These results indicate that $Li_{0.44}MnO_2$ nanowires show the good fast charge–discharge lithium storage property. These high current density performances are based on the nanowires structure, which achieve a higher surface area and shorter lithium ion diffusion length for fast lithium ion's diffusion. Moreover, the one-dimensional nanowires structure results in the relaxation of the volume change due to the lithium insertion/extraction, although the volume change under high current density condition is furious due to the quickly insertion/extraction by large amount of lithium ion. Fig. 7 shows the TEM images (a and b) and ED pattern (c) of the $Li_{0.44}MnO_2$ nanowires after the

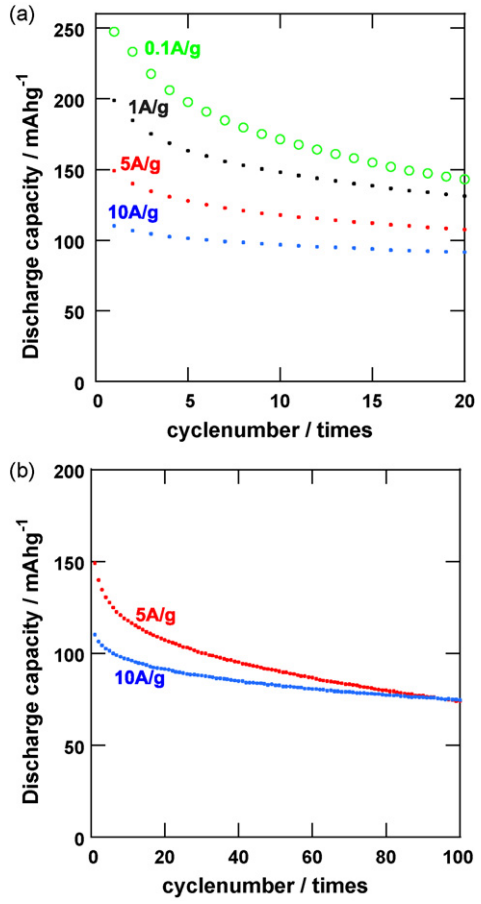

Fig. 6. The lithium storage characteristics of $Li_{0.44}MnO_2$ nanowires electrode. (a) Cycle performance of the $Li_{0.44}MnO_2$ nanowires electrode at various current densities up to 20 cycles (● 00.1 A g^{-1}, ● 1 A g^{-1}, ● 5 A g^{-1}, ● 10 A g^{-1}). (b) Cycle performance of the $Li_{0.44}MnO_2$ nanowires electrode at the high current densities condition up to 100 cycles (● 5 A g^{-1}, ● 10 A g^{-1}).

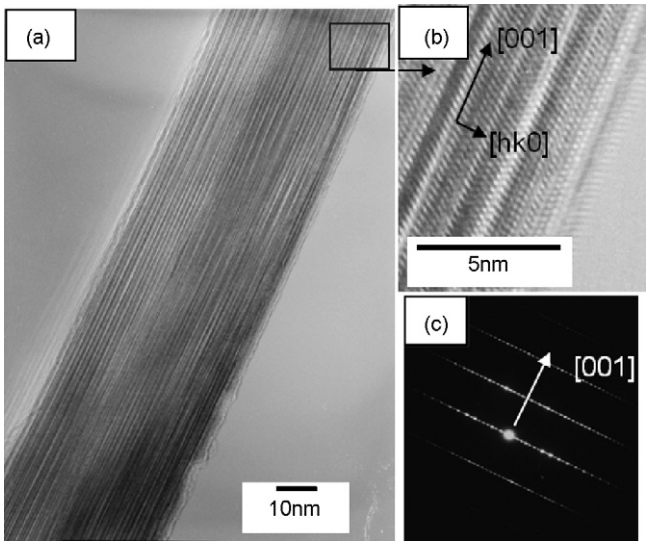

Fig. 7. (a) TEM image and (b) the high resolution TEM image of the nanowires after lithium storage measurement for 100 cycles at high current density condition of 10 A g^{-1}. The clear lattice image is similar to that of the $Li_{0.44}MnO_2$. (c) ED patterns.

100 cycles charge/discharge at the high current density condition of 10 A g^{-1}. We can see the one-dimensional nanowire structure without collapses. The single crystalline nature to one-dimensional direction in Fig. 7(b) and ED pattern in Fig. 7(c) are similar to those of before the charge/discharge cycling of $Li_{0.44}MnO_2$ nanowires electrodes. Even after the 100 cycles at 10 A g^{-1}, the single crystalline nanowire nature is still maintained. Therefore, the nanowires structure is suitable for the lithium ion battery under high current densities conditions.

4. Conclusions

The single crystalline $Li_{0.44}MnO_2$ nanowires is synthesized by ion exchange reaction from the sodium in $Na_{0.44}MnO_2$ nanowires to the lithium. The resultant $Li_{0.44}MnO_2$ nanowires indicate both the large specific charge–discharge capacity and good high current density charge–discharge performance based on the nanostructure nature for lithium ion battery.

Acknowledgment

This work was partially supported by the Development of High-performance Battery System for Next-generation Vehicles Project (Li-EAD Project) from the New Energy and Industrial Technology Development Organization (NEDO) of Japan.

References

[1] B. Gao, S. Sinha, L. Fleming, O. Zhou, Adv. Mater. 13 (2001) 816.
[2] Y. Idota, T. Kubota, A. Matsufuji, Y. Maekawa, T. Miyasaka, Science 276 (1997) 1395.
[3] P. Poizot, S. Laruelle, S. Grugeon, L. Dupont, J.-M. Tarascon, Nature 407 (2000) 496.
[4] H. Yamada, K. Tagawa, M. Komatsu, I. Moriguchi, T. Kudo, J. Phys. Chem. C 111 (2007) 8397.
[5] T. Kudo, Y. Ikeda, T. Watanabe, M. Hibino, M. Miyayama, H. Abe, K. Kajita, Solid State Ionics 152–153 (2002) 833.
[6] T. Watanabe, H.S. Zhou, I. Honma, J. Electrochem. Soc. 152 (2005) A1568.
[7] H. Kawaoka, M. Hibino, H.S. Zhou, I. Honma, Solid State Ionics 176 (2005) 621.
[8] J.Y. Luo, J.J. Zhang, Y.Y. Xia, Chem. Mater. 18 (2006) 5618.
[9] A.S. Aricò, P. Bruce, B. Scrosati, J.-M. Tarascon, W. Van Schalkwijk, Nat. Mater. 4 (2005) 366.
[10] H.S. Zhou, D. Li, M. Hibino, I. Honma, Angew. Chem. Int. Ed. 44 (2005) 797.
[11] A.R. Armstrong, G. Armstrong, J. Canales, R. García, P.G. Bruce, Adv. Mater. 17 (2005) 862.
[12] I. Moriguchi, R. Hidaka, H. Yamada, T. Kudo, H. Murakami, N. Nakashima, Adv. Mater. 18 (2006) 69.
[13] Y.G. Guo, Y.S. Hu, W. Sigle, J. Maier, Adv. Mater. 19 (2007) 2087.
[14] G.H. Dua, Z.Y. Yuan, G. Van Tendeloo, Appl. Phys. Lett. 86 (2005) 063113.
[15] W. Wang, C. Xu, G. Wang, Y. Liu, C. Zheng, Adv. Mater. 14 (2002) 837.
[16] R. Ma, Y. Bando, L. Zhang, T. Sasaki, Adv. Mater. 16 (2004) 918.
[17] M.M. Thackery, in: J.O. Besenhard (Ed.), Handbook of Battery Materials, Weily-VCH, 1999, pp. 293–321.
[18] M.M. Doeff, T.J. Richardson, L. Kepley, J. Electrochem. Soc. 143 (1996) 2507.
[19] E. Hosono, T. Kudo, M. Ichihara, I. Honma, H. Zhou, J. Power Sources 182 (2008) 349.
[20] A. Eftekhari, M. Kazemzad, F. Moztarzadeh, Mater. Res. Bull. 19 (2005) 1229.
[21] S. Hirano, R. Narita, S. Naka, Mater. Res. Bull. 19 (1984) 1229.
[22] F. Sauvage, L. Laffont, J.-M. Tarascon, E. Baudrin, Inorg. Chem. 46 (2007) 3289.
[23] E. Hosono, T. Kudo, I. Honma, H. Matsuda, H. Zhou, Nano Lett. 9 (2009) 1045.
[24] A.R. Armstrong, H. Huang, R.A. Jennings, P.G. Bruce, J. Mater. Chem. 8 (1998) 255.
[25] J. Akimoto, J. Awaka, Y. Takahashi, N. Kijima, M. Tabuchi, A. Nakashima, H. Sakaebe, K. Tatsumi, Electrochem. Solid-State Lett. 8 (2005) A554.
[26] M.M. Doeff, A. Anapolsky, L. Edman, T.J. Richardson, L.C. De Jonghe, J. Electorchem. Soc. 148 (2001) A230.
[27] Y.-S. Hu, L. Kienle, Y.-G. Guo, J. Maier, Adv. Mater. 18 (2006) 1421.
[28] D. Larcher, D. Bonnin, R. Cortes, I. Rivals, L. Personnaz, J.-M. Tarascon, J. Electrochem. Soc. 150 (2003) A1643.
[29] C.H. Jiang, M.D. Wei b, Z.M. Qi, T. Kudo, I. Honma, H.S. Zhou, J. Power Sources 166 (2007) 239.
[30] M. Okubo, E. Hosono, J. Kim, M. Enomoto, N. Kojima, T. Kudo, H.S. Zhou, I. Honma, J. Am. Chem. Soc. 129 (2007) 7444.